NASA/TM-20210014094

Modeling of the Influence of Thermally Grown Oxide (TGO) Layers on the Driving Forces in Environmental Barrier Coating Systems

Subodh K. Mital
The University of Toledo, Toledo, Ohio

Trenton M. Ricks, Steven M. Arnold, and Bryan J. Harder
Glenn Research Center, Cleveland, Ohio

April 2021

NASA STI Program . . . in Profile

Since its founding, NASA has been dedicated to the advancement of aeronautics and space science. The NASA Scientific and Technical Information (STI) Program plays a key part in helping NASA maintain this important role.

The NASA STI Program operates under the auspices of the Agency Chief Information Officer. It collects, organizes, provides for archiving, and disseminates NASA's STI. The NASA STI Program provides access to the NASA Technical Report Server—Registered (NTRS Reg) and NASA Technical Report Server—Public (NTRS) thus providing one of the largest collections of aeronautical and space science STI in the world. Results are published in both non-NASA channels and by NASA in the NASA STI Report Series, which includes the following report types:

- TECHNICAL PUBLICATION. Reports of completed research or a major significant phase of research that present the results of NASA programs and include extensive data or theoretical analysis. Includes compilations of significant scientific and technical data and information deemed to be of continuing reference value. NASA counter-part of peer-reviewed formal professional papers, but has less stringent limitations on manuscript length and extent of graphic presentations.

- TECHNICAL MEMORANDUM. Scientific and technical findings that are preliminary or of specialized interest, e.g., "quick-release" reports, working papers, and bibliographies that contain minimal annotation. Does not contain extensive analysis.

- CONTRACTOR REPORT. Scientific and technical findings by NASA-sponsored contractors and grantees.

- CONFERENCE PUBLICATION. Collected papers from scientific and technical conferences, symposia, seminars, or other meetings sponsored or co-sponsored by NASA.

- SPECIAL PUBLICATION. Scientific, technical, or historical information from NASA programs, projects, and missions, often concerned with subjects having substantial public interest.

- TECHNICAL TRANSLATION. English-language translations of foreign scientific and technical material pertinent to NASA's mission.

For more information about the NASA STI program, see the following:

- Access the NASA STI program home page at http://www.sti.nasa.gov

- E-mail your question to help@sti.nasa.gov

- Fax your question to the NASA STI Information Desk at 757-864-6500

- Telephone the NASA STI Information Desk at 757-864-9658

- Write to:
  NASA STI Program
  Mail Stop 148
  NASA Langley Research Center
  Hampton, VA 23681-2199

NASA/TM-20210014094

Modeling of the Influence of Thermally Grown Oxide (TGO) Layers on the Driving Forces in Environmental Barrier Coating Systems

Subodh K. Mital
The University of Toledo, Toledo, Ohio

Trenton M. Ricks, Steven M. Arnold, and Bryan J. Harder
Glenn Research Center, Cleveland, Ohio

National Aeronautics and
Space Administration

Glenn Research Center
Cleveland, Ohio 44135

April 2021

Acknowledgments

This work was supported under the NASA's Transformational Tools and Technologies (TTT) project within the Aeronautics Research Mission Directorate.

This report contains preliminary findings, subject to revision as analysis proceeds.

This work was sponsored by the Transformative Aeronautics Concepts Program.

Level of Review: This material has been technically reviewed by technical management.

Available from

NASA STI Program
Mail Stop 148
NASA Langley Research Center
Hampton, VA 23681-2199

National Technical Information Service
5285 Port Royal Road
Springfield, VA 22161
703-605-6000

This report is available in electronic form at http://www.sti.nasa.gov/ and http://ntrs.nasa.gov/

Modeling of the Influence of Thermally Grown Oxide (TGO) Layers on the Driving Forces in Environmental Barrier Coating Systems

Subodh K. Mital
The University of Toledo
Toledo, Ohio 43606

Trenton M. Ricks, Steven M. Arnold, and Bryan J. Harder
National Aeronautics and Space Administration
Glenn Research Center
Cleveland, Ohio 44135

Abstract

Environmental barrier coatings (EBC) are an enabling technology for the successful application of ceramic matrix composites (CMCs) in air-breathing gas turbine engines. EBCs are susceptible to several failure modes including oxidation/delamination, recession, chemical attack and dissolution, thermomechanical degradation, erosion, and foreign object impact damage in a combustion environment. Spallation of environmental barrier coating (EBC), induced by a thermally grown oxide (TGO) layer, is a key EBC failure mode. The TGO layer, resulting from steam oxidation, grows either from a silicon bond coat layer (if present) or from a silicon carbide (SiC) based substrate itself. The TGO layer evolves (i.e., thickness increases with time) as water vapor and oxygen gradually diffuse through the EBC, and the EBC spalls off once the TGO layer reaches some critical thickness. The critical thickness of the TGO layer for failure is in the range of 20 to 30 μm, with the actual value depending upon exposure temperature, microstructure, etc. Current work at NASA Glenn Research Center, under the Transformative Tools and Technology (TTT) subproject is aimed at addressing associated failure modes in EBC systems and developing robust analysis tools to aid in the design/analysis of these systems. The objective of the current work is to conduct a sensitivity study to examine the influence of uniformly and non-uniformly grown oxide layers on the associated driving forces leading to spallation of the EBC when subjected to isothermal loading. The effect of damage in the TGO layer on the resulting stress states is also assessed both in uniform and non-uniform TGO layers.

Introduction

Silicon carbide fiber-reinforced silicon carbide matrix (SiC/SiC) composites are advanced ceramic matrix composites (CMCs) that are prime candidates for hot section structural components of gas turbine engines. CMCs offer many advantages as compared to metallic materials. SiC/SiC composites have about one-third the mass density and approximately 200 °C higher operating temperature as compared to their metallic counterparts. The higher operating temperature improves thermal efficiency (i.e., reduction in cooling air), higher propulsive efficiency and reduction in NOx emissions. SiC/SiC composites are currently being used in high-pressure turbine shrouds of CFM International Leading Edge Aviation Propulsion (LEAP) engines. Similar materials are slated to be used in inner and outer combustor liners as well as high-pressure turbine nozzles and shrouds in the GE9X engine, expected to enter service in near future (Ref. 1). It is expected that SiC/SiC composites will then be used for rotating components such as turbine blades which will produce much lower centrifugal forces thus requiring much lighter disks.

Despite this progress, many challenges remain for the insertion of CMCs into commercial use. For example, SiC turns into silica (SiO_2) in the presence of oxygen (combustion air). Then, in the presence of water vapor, which is a by-product of combustion, silica coverts into a gaseous $Si(OH)_4$ thus leading to rapid recession of SiC material. Thus, it is very important to protect SiC from water vapor in a combustion environment. An external environmental barrier coating (EBC) is applied to the CMC systems to provide protection from oxygen and water-vapor and thus provide long-term stability (Ref. 2). Additionally, EBCs provides a thermal gradient to exist on the CMC/EBC system further increasing its use temperature.

Failure of the EBC will lead to a rapid reduction in CMC component life. There are many possible failure modes of EBCs such as water vapor-induced recession, oxidation in oxygen and high temperature environment due to water vapor leading to growth of thermally-grown oxide (TGO) layer, degradation due to calcium-aluminum-magnesium silicates (CMAS) deposits, degradation due to thermo-mechanical cyclic loads, and damage due to impact by foreign objects (FOD) (Ref. 2). However, in this work, only the influence of TGO growth and its impact on thermomechanical stresses within the EBC system will be examined. In real situations, many of these factors are present simultaneously.

It is known that both Si and SiC are oxidized primarily by water vapor when exposed to an oxygen-rich and high temperature environment. Water permeates through the top EBC layer and reacts with the underlying substrate (e.g., Si or SiC). As a result, it forms a layer of SiO_2 scale known as thermally grown oxide (TGO) at the interface. Tests have shown that the EBC fails or spalls once this TGO reaches a critical thickness somewhere in the range of 20 to 30 μm. Although not addressed here, one way to extend the life of EBC systems is to somehow reduce the TGO growth rate. Studies at NASA Glenn Research Center are currently investigating whether TGO growth rates can be reduced by adding some modifiers and thus changing the chemistry of the constituents (Ref. 3).

Environmental Barrier Coating Systems

EBCs can be classified into two categories based on their upper use temperature. One is a low temperature system which consists of three basic layers: a top layer of a rare earth silicate EBC, a middle silicon (Si) bond coat layer, and the third (or base) CMC substrate. Since silicon melts at 1410 °C, the upper use temperature of these category of coating systems is limited to 1315 °C (2400 °F). Most of these systems are some variant of the so-called second-generation EBC systems developed under the sponsorship of NASA's Ultra Efficient Engine Technology (UEET) program (Ref. 4). When there is a growth of the TGO layer from the silicon bond coat, there are a total of four-layers: substrate, Si bond coat layer, TGO layer, and the rare-earth silicate based top-layer. Consequently, the low temperature system is referred to as a four-layer system. The other system is a higher temperature system where the Si bond coat layer is removed as it limits the use temperature of the coating system. The use temperature of these initial EBC/CMC systems can be greater than 1315 °C (> 2400 °F). As before, with the growth of the TGO layer, there are a total of three-layers: the substrate, the TGO layer that grows out of the substrate, and the EBC. Consequently, this higher temperature system is referred to as a three-layer system.

The objective of this paper is to analyze both a three-layer (EBC/TGO/Substrate) high temperature system and a four-layer (EBC/TGO/Bond Coat/Substrate) low temperature system with uniform and non-uniform TGO layers for two TGO layer thicknesses subject to isothermal cool-down from an assumed stress free high-temperature to room temperature. Resulting stresses in the layers are assessed for an undamaged and damaged TGO (variable vertical crack spacings). The results provide a means to estimate the in-situ strength of the pristine TGO material and likely locations of EBC delamination. In these analyses, time effects (i.e., TGO growth rates, creep of various materials, etc.) and volumetric effects due to the phase change of the materials as well as free edge effects were not considered. Therefore, these results should be considered qualitative and not quantitative.

Analyses

In a previous work (Ref. 5), NASA's Higher-Order Theory for Functionally Graded Materials (HOTGM) micromechanics code (Ref. 6) was used to identify and assess the driving forces as the TGO thickness evolved in the three-layer higher-temperature EBC system. That work has been extended in this paper to include additional factors, such as damage in the TGO layer and anisotropy in the substrate. Previously, and herein the SiC/SiC substrate was replaced by a Hexoloy monolithic ceramic in the analyses (since this is typically used during system testing). It has been observed (but not shown here) that use of monolithic transversely isotropic, or anisotropic, substrates have virtually no effect on the stresses in the EBC or the TGO layer. Consequently, herein the substrate was taken to be an isotropic monolithic material. The EBC system was subjected to isothermal cooling from an assumed stress-free temperature of 1482 to 38.7 °C. These analyses only provide a qualitative representation of the stress state (i.e., driving forces) as only elastic, time-independent analyses were performed as a first-order approximation and free edge effects and volumetric strains arising due to the phase change of the materials were ignored. Constituent properties shown in Table I have also been assumed to be isotropic and independent of temperature. The three-layer and four-layer EBC systems with two TGO thicknesses (4 and 16 μm) have been analyzed in this paper. Realistic EBC systems have a non-uniform thickness. To evaluate the effect of non-uniformity of the TGO, two non-uniform configurations were analyzed. In addition, vertical cracks were simulated in the TGO layer at an 80, 40, 20, or 10 μm spacing and, the change in the resulting stress states were evaluated. Experimentally, EBC systems have been observed to have vertical cracks spaced at around 10 μm on average in the TGO layer regardless of TGO thickness. Consequently, this spacing can be used to provide an estimate of the in-situ tensile strength of the TGO material. Any residual stresses that arise due to processing have not been explicitly accounted for in this study but can be assumed to be included in the characterized strength values.

TABLE I.—CONSTITUENT ISOTROPIC THERMOELASTIC PROPERTIES

Material	Thickness, mm	Modulus, GPa	Poisson ratio	CTE, $x10^{-6}$ K^{-1}
$Yb_2Si_2O_7$ (EBC)	0.175	200	0.27	4.5
SiO_2 (TGO)	varies	35	0.17	10
Si (Bond Coat)	0.075	97	0.21	4.5
Hexoloy SiC (Substrate)	[a]3	400	0.17	5.25

[a]Initial thickness assuming no TGO

A schematic of the specific three-layer EBC system investigated here is shown in Figure 1(a). Wherein the overall width (L = 10 mm) and thickness (H = 3.175 mm) of the specimen are shown; the width was chosen to ensure uniform fields away from the free edge. The primary loading is that due to uniform isothermal cooling, where the temperature varies linearly from the stress-free reference temperature of T = 1482 °C (2700 °F) to the final temperature of 38.7 °C (102 °F). Constituent deformation behavior is assumed to follow Hooke's law. The thermo-elastic properties of all three constituent materials ($Yb_2Si_2O_7$ - EBC, SiO_2 TGO, and Hexoloy SiC substrate) are all assumed to be isotropic and are given in Table I. The properties are assumed to be temperature independent, even though the thermal properties are likely to be highly temperature dependent. Finally, in all simulations the total system thickness, H ($t_{EBC} + t_{TGO} + t_S$), was held fixed at 3.175 mm; thus, as the TGO thickness increases substrate thickness commensurately decreases (or is "consumed") as observed experimentally. All analyses performed herein involve 2-D plane stress elements (CPS4) using the ABAQUS general-purpose finite element program (Ref. 7). Symmetry boundary conditions were applied at the plane $x_1 = 0$ to reduce the computational domain. The normal stress in the 1-direction is referred to as in-plane stress (σ_{11}), which could cause vertical cracking to occur, while the normal stress in the 2-direction is referred to as out-of-plane or "peel" stress (σ_{22}), which could cause delamination. Whereas, the shear stress in the 1-2 plane (σ_{12}) may drive the delamination along the layer boundaries.

In case of the four-layer system, there is a silicon bond coat with an initial thickness of 75 μm and this bond coat converts to TGO with time, the thickness of TGO layer grows and the thickness of bond coat layer reduces. A schematic of the four-layer system is shown in Figure 1(b).

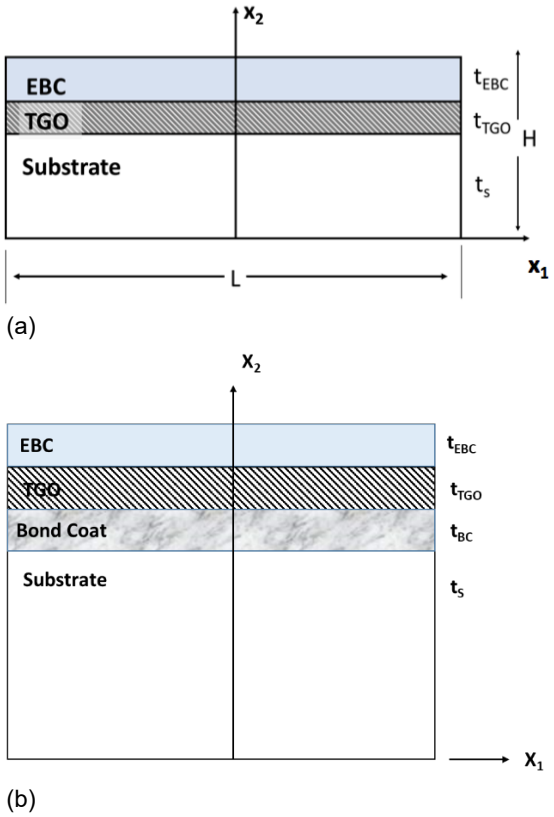

Figure 1.—Schematic showing the three-layer EBC system (a). Schematic showing the four-layer EBC system (b).

Results

Three-Layer High Temperature System

Uniform Layers

A variety of simulations were performed to assess the influence of TGO growth, i.e., thickness increase of a continuous uniform TGO layer, on the stress state of a three-layer EBC/TGO/Substrate system after thermal cooldown. This system was analyzed using two TGO thicknesses: a 4 μm (thin) and 16 μm (thick) TGO layer. The results for only the thick TGO layer are presented here for the sake of brevity and are similar to those for the thin TGO layer. The maximum in-plane stress in a thick TGO layer as a function of vertical crack spacing is shown in Figure 2(a), for five conditions: an undamaged TGO layer as well as TGO layers with an 80, 40, 20, or 10 μm crack spacing. Vertical cracks (or damage) in the TGO layer were simulated by replacing appropriate columns of TGO elements with near-zero stiffness elements. Figure 2(b) to (e) show the TGO layer mesh discretization along with the corresponding in-plane stress state for the undamaged and damaged TGO with 80, 40, 20, and 10 μm crack spacings, respectively. Clearly, in the case of no damage (cracks) a uniform in-plane stress value of approximately 250 MPa develops within the TGO. As shown in Figure 2(c), for crack spacing of 80 μm, the in-plane stress between cracks can also reach values as high as 250 MPa (i.e., as individual cracks do not “feel” each other). As crack spacing decreases, the in-plane stress between cracks within the interior of the TGO reduce while that along the top and bottom layer edge remain elevated due to crack interaction and boundary effects. However, as shown in Figure 2, at large crack spacings (>20 μm), significant tensile in-plane stresses (greater than 200 MPa) can develop and would result in further cracking of the TGO layer in between existing cracks. However, once the average crack spacing approaches 10 μm, there is not enough distance in the pristine TGO material to enable development of significant tensile in-plane stress to cause further cracking. This lack of significant distance for stress development is very similar to the well-known shear-lag theory in fiber-reinforced composites. Consequently, given that the experimentally observed crack spacing at the time of coating failure is around 10 μm in the TGO layer, one can estimate that according to the current idealization the in-situ strength of the pristine TGO material should be apparently around 200 MPa. The exact magnitude is unknown as the stress analysis results are dependent upon the assumed mesh density, material properties, and flaw population thus the qualitative nature of the current study.

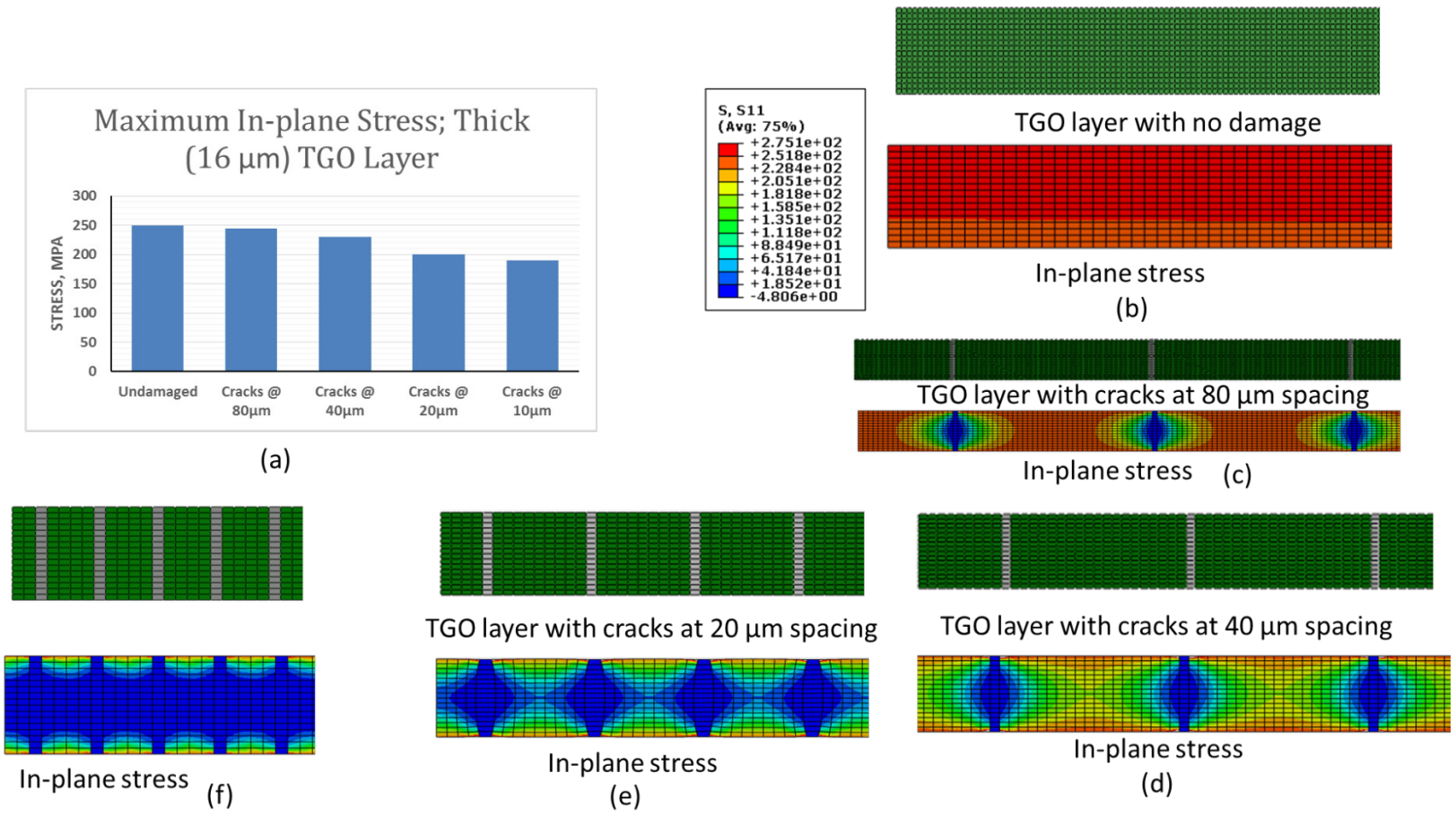

Figure 2.—Maximum in-plane stress in the uniform thick TGO three-layer system (elements representing cracks are shown in gray). (a) Maximum in-plane stress vs. crack spacing. (b) TGO layer discretization with no damage and the resulting in-plane stress state. TGO layer with a crack spacing of (c) 80 µm, (d) 40 µm, (e) 20 µm, and (f) 10 µm and the corresponding resulting in-plane stress contours.

Figure 3 shows that when there was no damage assumed in the TGO layer, the in-plane stresses within the TGO layer were significant and independent of TGO thickness, while peel and shear stresses were minimal. However, when vertical cracking has saturated at 10 μm spacing, the maximum in-plane stress magnitude slightly decreased (although located only along the layer edges), but now significant peel and shear stresses were present (as shown in Figure 4). The peel and shear stresses also increased with increasing TGO thickness; thus, suggesting the possibility of delamination initiation and propagation at the TGO layer interface near the damage (crack) locations. In such a scenario, it is possible that the increase in shear stress could cause vertical cracks to turn and link with neighboring cracks before leading to EBC spallation.

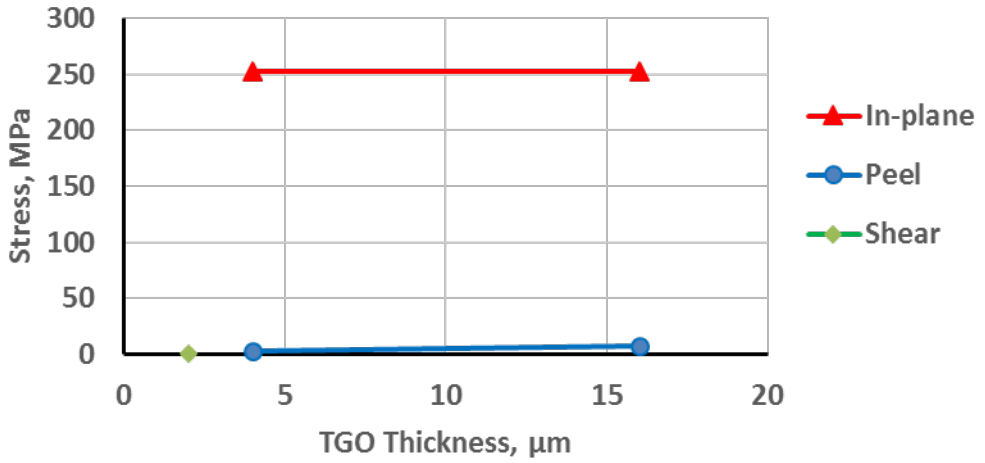

Figure 3.—Maximum stresses in the uniform TGO layer, no TGO damage.

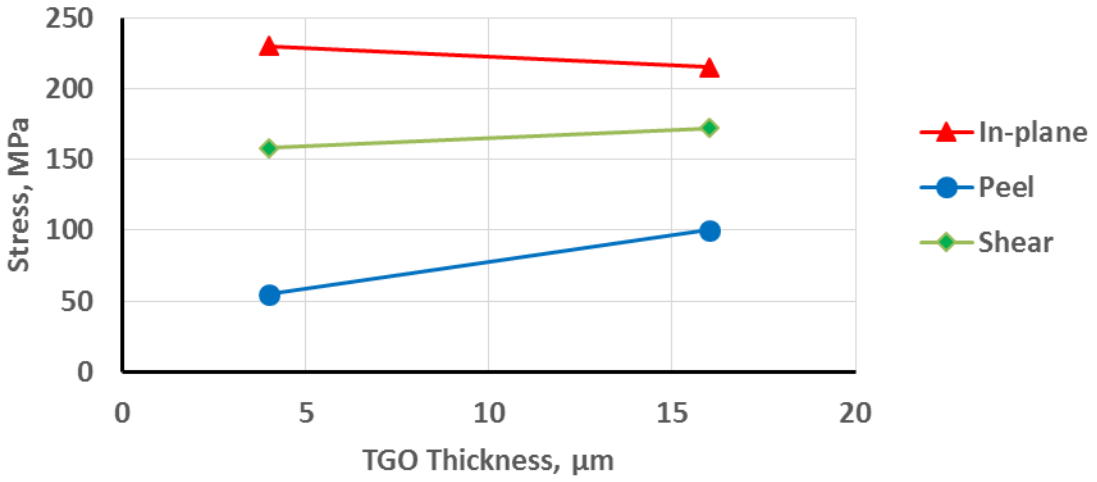

Figure 4.—Maximum stresses in the uniform, damaged, TGO layer, 10 μm vertical crack spacing.

Since in-plane stresses are highest at the interface of the TGO with EBC or the substrate as seen in Figure 2, vertical cracks are likely to initiate from there and propagate toward the center of the TGO layer. To investigate this, an FEA mesh with partial vertical cracks were introduced at 10 μm spacing. Analyses were performed with three TGO thicknesses 4, 6, and 8 μm. Results, shown in Figure 5, indicate that in-plane stress at the tip of the partial cracks is very high, in excess of 300 MPa. Thus, the partial cracks are likely to propagate and coalesce into a full vertical crack almost instantaneously.

Non-Uniform Layers

As mentioned before, EBC layers are rarely uniform because of the way they are deposited onto a substrate. TGO layer growth is also rarely uniform as well. In prior work (Ref. 5), TGO layer thickness non-uniformity was modeled as shown in Figure 6, wherein, a parameter R was defined as d/t_{TGO}. Consequently, severity of the non-uniformity was modeled by changing this parameter R. Thus, R = 0 represents islands of TGO (the most severe non-uniformity) and R = 1 represents a smooth (or uniform) TGO layer. In this work, four cases have been examined, i.e., R = 0, 0.75 and 0.875, which represents a minor non-uniformity, and R = 1. W_{TGO} was assumed to be 120 μm, and W_{BC} was assumed to be 60 μm consistent with previous work (Ref. 5).

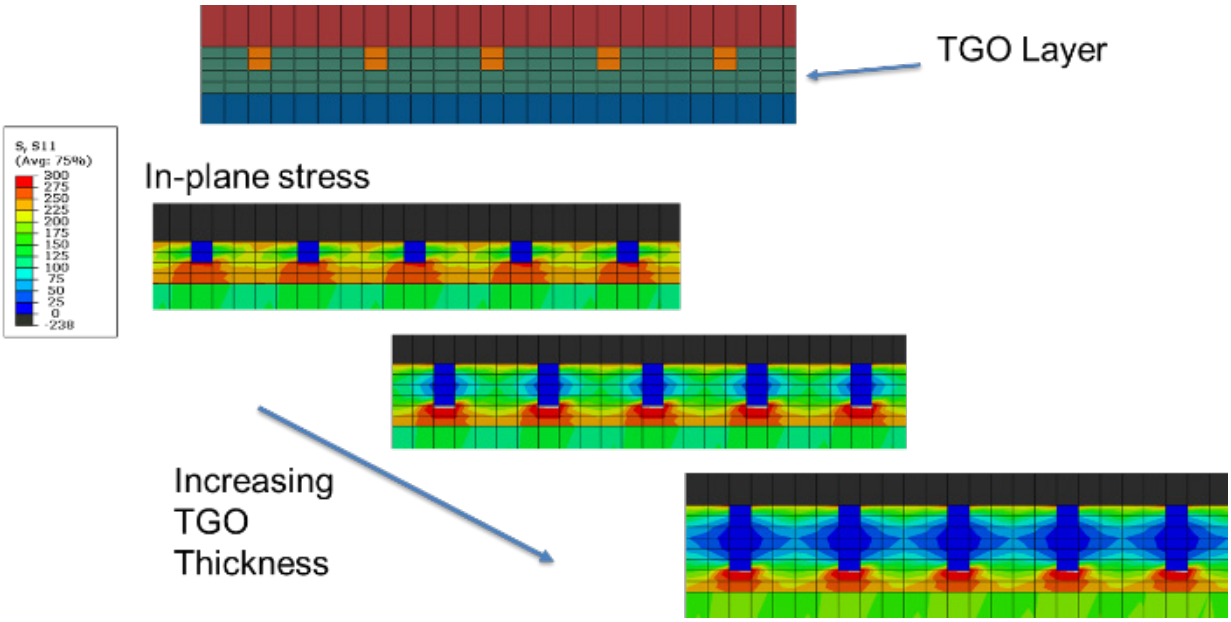

Figure 5.—Geometry (top) and contours of in-plane stress (bottom) for full and partial vertical cracks in the TGO layer with increasing thickness.

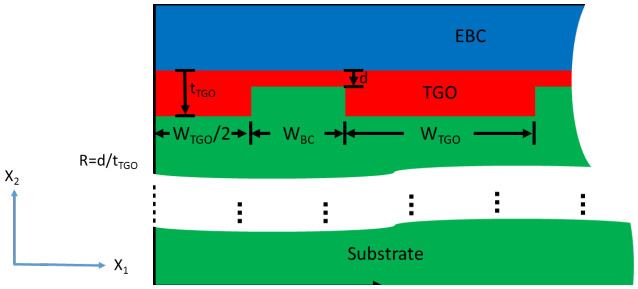

Figure 6.—Schematic showing discontinuous TGO layer geometry.

As before, this system (with R = 0.75) was also analyzed for two maximum TGO thicknesses: a 4 μm (thin) and a 16 μm (thick) TGO layer. The results for only the thick TGO layer are presented here for the sake of brevity as thin TGO layer results were qualitatively similar. Figure 7(a) shows the maximum in-plane tensile stress vs. the crack spacing in the TGO layer. Figure 7(b) to (f) show the TGO layer mesh discretization along with the corresponding in-plane stress state for the undamaged and damaged TGO with 80, 40, 20, and 10 μm crack spacings, respectively. As in the uniform case, higher in-plane stresses exist when cracks were spaced further apart. As shown in Figure 7(c), when cracks are at 80 μm spacing, high in-plane stresses will develop as if cracks are not influencing each other. Although, the starting maximum in-plane stress in the undamaged TGO with non-uniformity was slightly higher (2 percent) than the stress in the uniform TGO layer case. Note that in Figure 7(b) to (f), the left edge of the contour plots does not necessarily correspond to the centerline (plane of symmetry) of the FEA mesh. Also, for the case when the crack spacing was 40 μm, see Figure 7(d), the vertical crack happens to align with the edge of the non-uniformity; whereas for other spacing the vertical cracks are on either side of the edge of the non-uniformity. Again, the cracks interact at 40 μm crack spacing to cause roughly an 8 percent decrease in the maximum in-plane stress while at 10 μm spacing, the stress was reduced by approximately 24 percent (185 to 190 MPa). As before, some critical distance is needed (akin to shear-lag theory) for enough in-plane stresses to develop to cause continued cracking. In the case of non-uniform TGO layers, it is apparent that both peel and shear stresses are significant, whether the TGO is undamaged (see Figure 8) or damaged (see Figure 9). Note, in both figures the dashed lines are associated with the thin TGO layer while the solid is associated with the thick TGO layer. Also, the stresses plotted are maximum values and therefore aren't necessarily associated with the same location. Comparing Figure 8 and Figure 9 for R = 1 (uniform TGO layer case), in the presence of damage (cracks) (see Figure 9) significant peel and shear stresses were generated. And, that these stresses increased as non-uniformity of the TGO layer was increased regardless of TGO thickness. Figure 8 shows that even at slight non-uniformity, significant peel stresses develop that can cause initiation of delamination or horizontal cracks (as they exceed the 200 MPa strength determined earlier). The magnitude of peel stress is independent of the severity of non-uniformity as it is driven by the property mismatch between TGO and substrate within the TGO layer itself. A shear stress is also induced with this peel stress and it rises in magnitude significantly as the TGO thickness increases (or grows). It is postulated that at a critical TGO thickness the shear stress will become high enough to propagate the horizontal crack (delamination) induced by the peel stress. In-plane and peel stresses are independent of the TGO thickness. However, in the presence of damage and non-uniformity (as shown in Figure 9), there are significant shear and peel stresses for delamination to initiate and propagate causing spallation of the coating (particularly when the TGO becomes thick, e.g., 16 μm (solid curves).

Consequently, the layer non-uniformity and presence of cracks, both of which are present in real systems, increase the peel and shear stresses, thereby increasing the likelihood of delamination initiation and propagation at the highest stress locations. The presence of damage increases the stresses that are present due to non-uniformity and thus increasing the likelihood of failure. However, the presence of non-uniformity itself is still the dominant factor influencing the magnitude of peel and shear stresses. To predict actual locations of failure, one has to take into account the resistance (strength) of different layers as well as bond strength between layers. Knowledge of resistance will also be necessary to predict the critical TGO thickness that will result in spallation or failure. This work has only addressed the driving forces or the resulting stresses in the TGO layer. Real cracks with crack growth, stress intensity etc. are needed along with material resistance curves to predict the critical parameters. However, in the current study actual cracks are not there but only reduced stiffness elements to mimic stiffness reduction/stress relief due to cracks are present. Additionally, temperature dependent material properties along with the time effects not accounted for, the current results should be looked at in a qualitative sense.

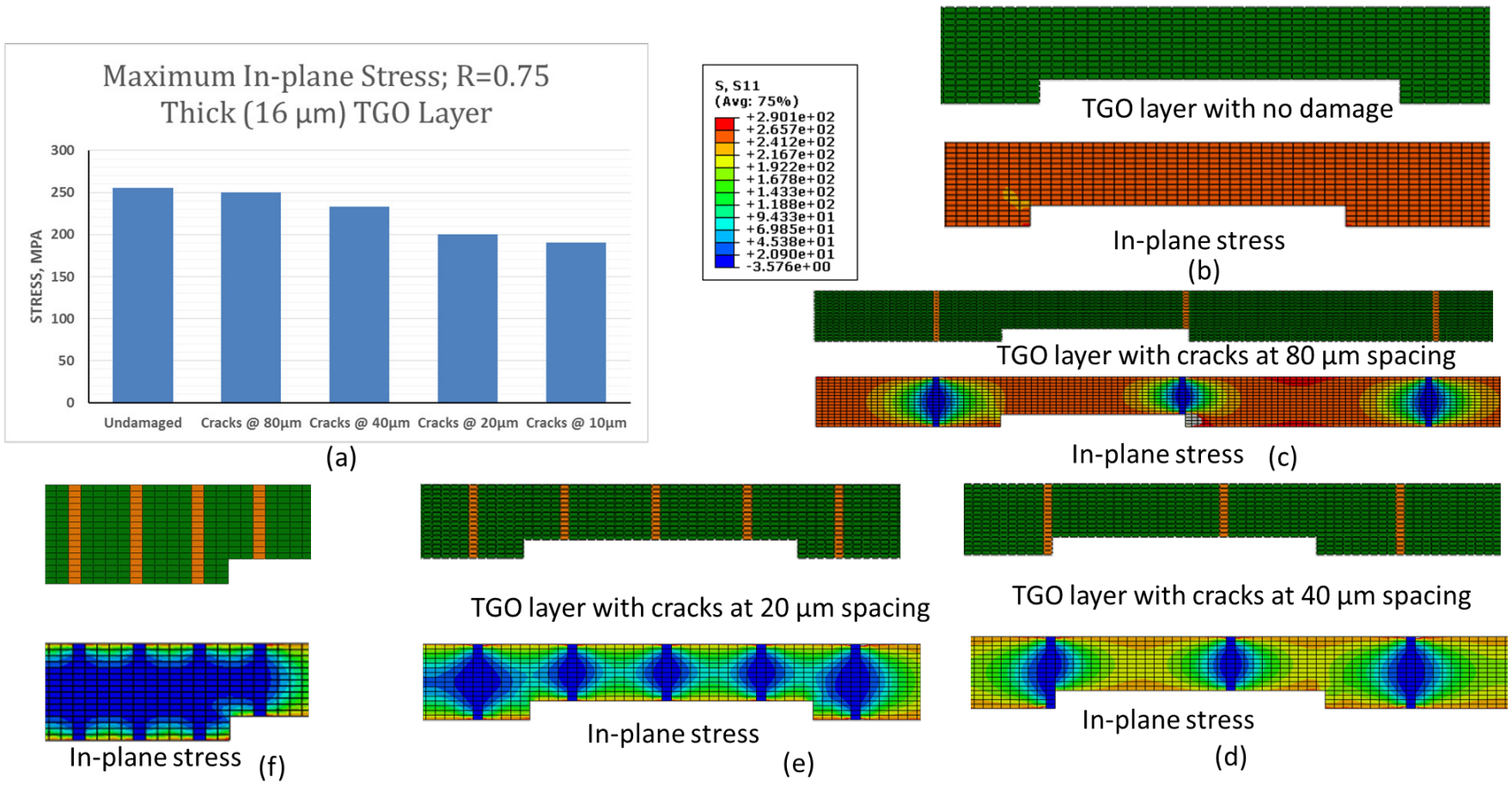

Figure 7.—Maximum in-plane stress in the non-uniform thick TGO layer with R = 0.75 (elements representing cracks are shown in orange). (a) Maximum in-plane stress vs. crack spacing. (b) TGO layer with no damage and the resulting in-plane stress state. TGO layer with crack spacing at (c) 80 µm, (d) 40 µm, (e) 20 µm, and (f) 10 µm and the corresponding resulting in-plane stress contours.

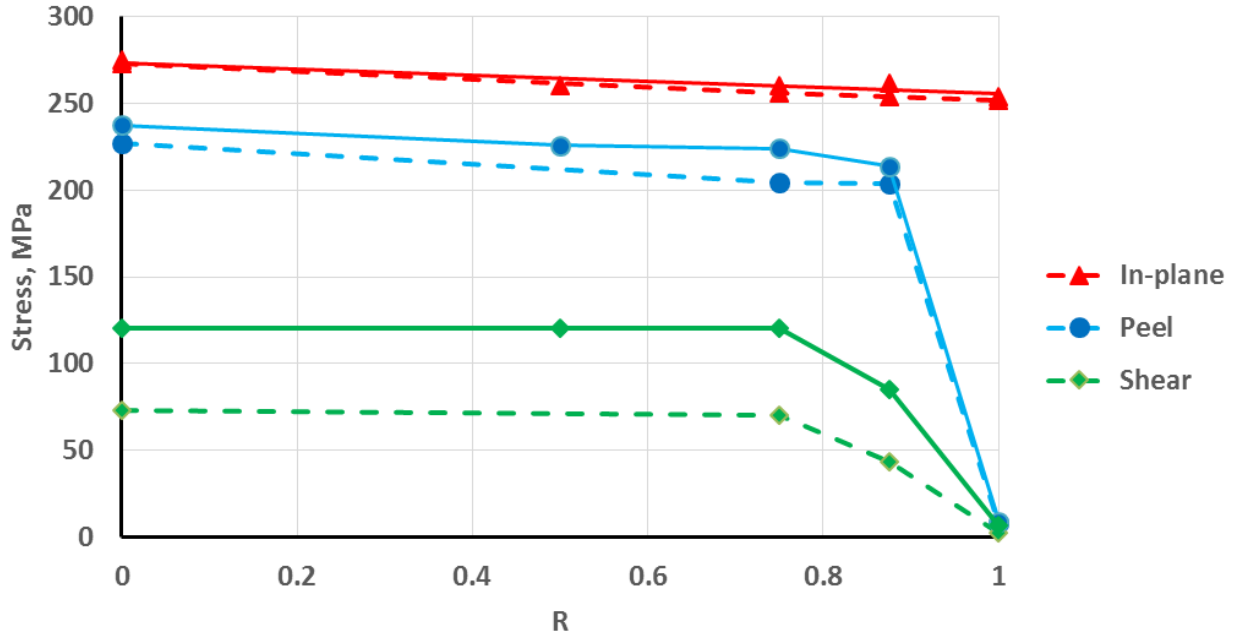

Figure 8.—Maximum stresses in the TGO layer. No damage assumed in TGO layer. Solid lines represent thick (16 μm) TGO and dash line represent thin (4 μm) TGO.

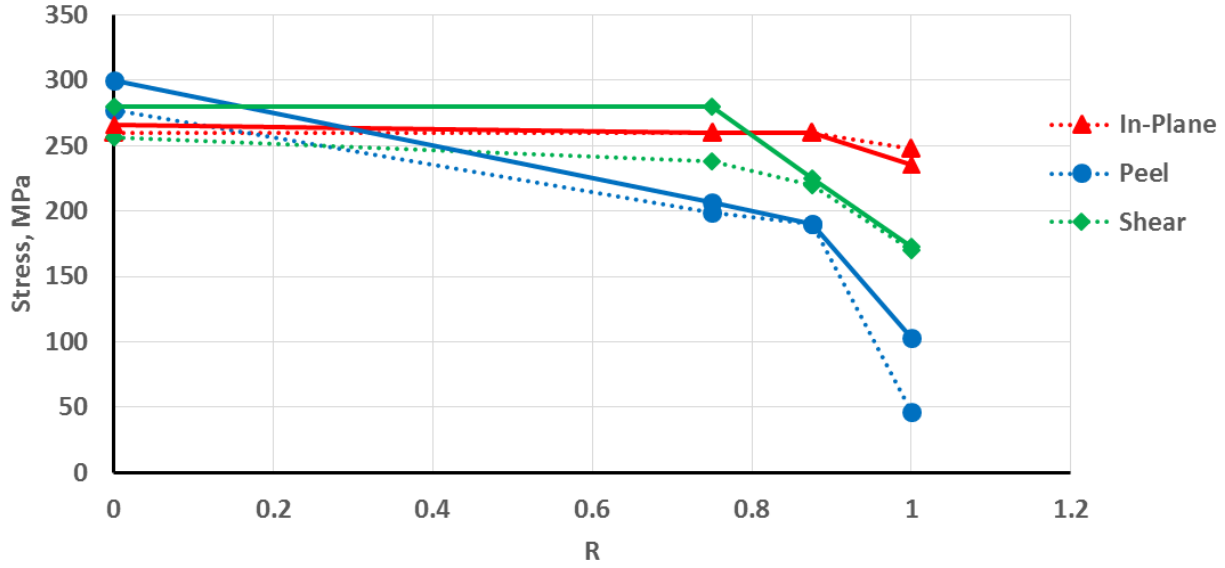

Figure 9.—Maximum stresses in TGO layer. Vertical cracks in TGO layer at a 10 μm spacing. Solid lines represent thick (16 μm) TGO and dash lines represent thin (4 μm) TGO.

Four-Layer Low Temperature System

Uniform Layers

For this system, similar analyses were performed for the growth of TGO to assess the stress state of a four-layer (EBC/TGO/Bond Coat/Substrate) system. This system was also analyzed for a thermal cooldown down as before primarily for two thicknesses 4 μm (thin) and 16 μm (thick) TGO layer. The results for thick TGO layer analyses are shown here (results for thin TGO layer were very similar) for comparison to the results obtained from the analyses of three-layer system. Figure 10(a) shows maximum in-plane stress as a function of vertical crack spacing as well as in-plane stress contours for an undamaged TGO layer and TGO layers with an 80, 40, 20, and 10 μm crack spacing in Figure 10(b) to (f). As before, vertical cracks (or damage) in the TGO layer were simulated by replacing appropriate columns of TGO elements with near-zero stiffness elements. For the case of undamaged TGO layer, a uniform in-plane stress value of approximately 260 MPa develops within the TGO layer. At higher crack spacing values (> 40 μm), there is no interaction between the cracks and the stress value reaches as high as 260 MPa possibly resulting in further cracking of TGO layer. At crack spacing below 20 μm or so, cracks start interacting with each other. As crack spacing nears 10 μm (experimentally observed value), there is lack of enough distance for significant tensile stresses to develop in the TGO layer. As before, it is estimated that the tensile strength of pristine TGO materials has be at least 200 MPa. As mentioned previously, exact magnitude is unknown because of the qualitative nature of current evaluations.

Figure 11 shows that when there was no damage assumed in the TGO layer, the in-plane tensile stresses within TGO layer were significant and relatively independent of TGO layer thickness, while peel and shear stresses are almost zero. However, as damage in the form of vertical cracks is introduced in the TGO layer, in-plane tensile stress decreases slightly. There is also a slight increase in the in-plane tensile stress as the TGO layer thickness grows. However, significant peel and shear stresses develop in the presence of vertical cracks (as shown in Figure 12). The peel and shear stresses also increased with increasing TGO thickness; thus, suggesting the possibility of delamination initiation and propagation at the TGO layer interface near the damage (crack) locations. In such a scenario, it is possible that the increase in shear stress could cause vertical cracks to turn and link with neighboring cracks before leading to EBC spallation. These observations are very similar to what was observed in the case of three-layer EBC system.

Non-Uniform Layers

As discussed previously, in real applications, EBC layers are almost never uniform. The way layers are deposited, the way they grow with time usually results in non-uniform layer thicknesses. TGO layer thickness non-uniformity was modeled as shown in Figure 13, wherein, a parameter R was defined as d/t_{TGO}. Consequently, severity of the non-uniformity can be modeled by changing this parameter R. Thus, R = 0 represents true islands of TGO material (the most severe non-uniformity) and R = 1 represents a smooth (or uniform) TGO layer. Here, three cases of non-uniform TGO layer have been examined, i.e., R = 0, 0.75 and R = 1. Again, W_{TGO} was assumed to be 120 μm, and W_{BC} was assumed to be 60 μm consistent with previous analyses for three layer systems.

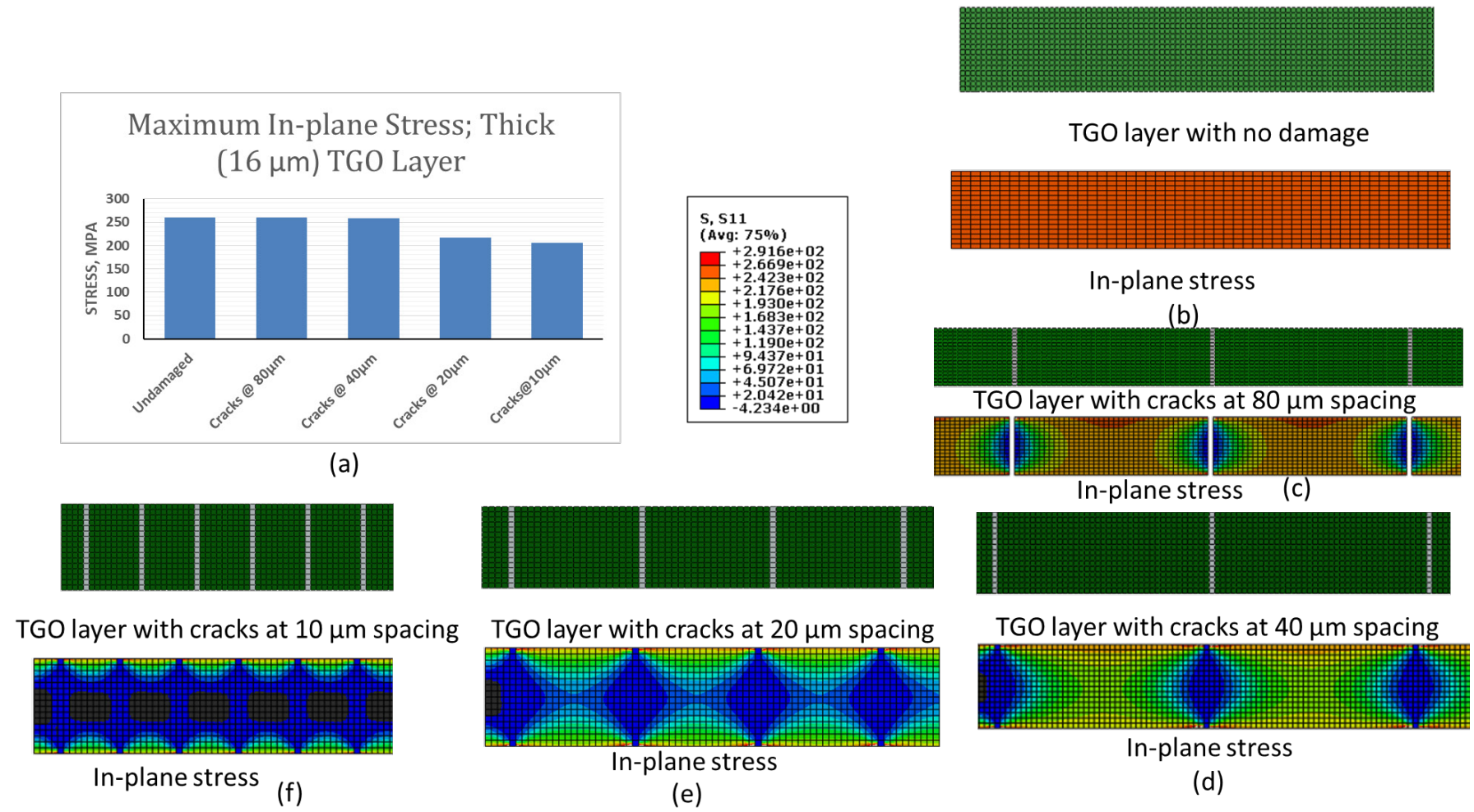

Figure 10.—Maximum in-plane stress in the uniform thick TGO four-layer system (elements representing cracks are shown in gray). (a) Maximum in-plane stress vs. crack spacing. (b) TGO layer discretization with no damage and the resulting in-plane stress state. TGO layer with a crack spacing of (c) 80 µm, (d) 40 µm, (e) 20 µm, and (f) 10 µm and the resulting in-plane stress states.

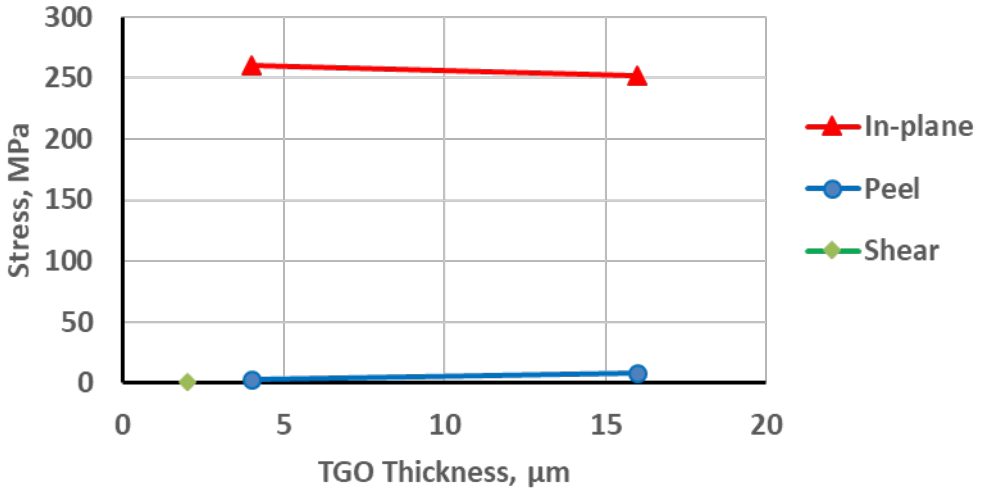

Figure 11.—Maximum stresses in the uniform TGO layer, no TGO damage.

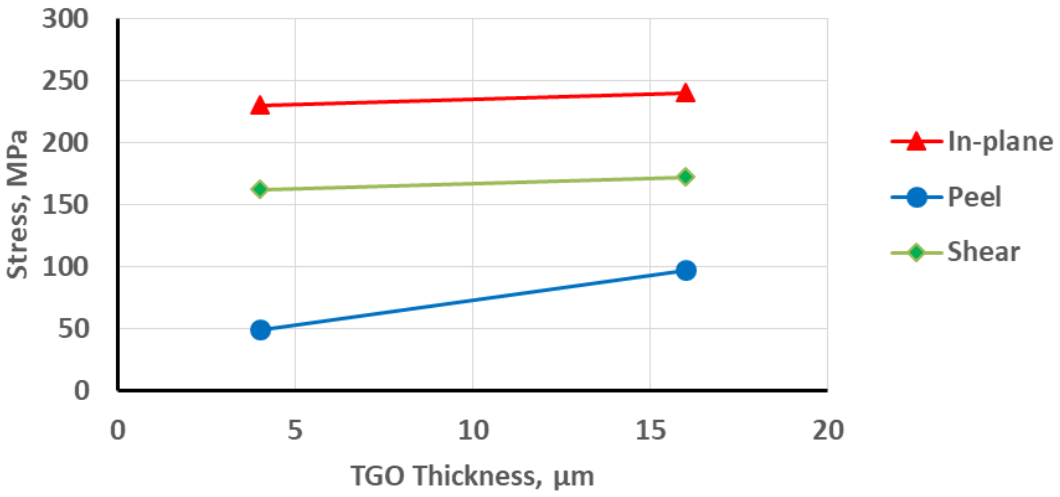

Figure 12.—Maximum stresses in the uniform, damaged, TGO layer, 10 µm vertical crack spacing.

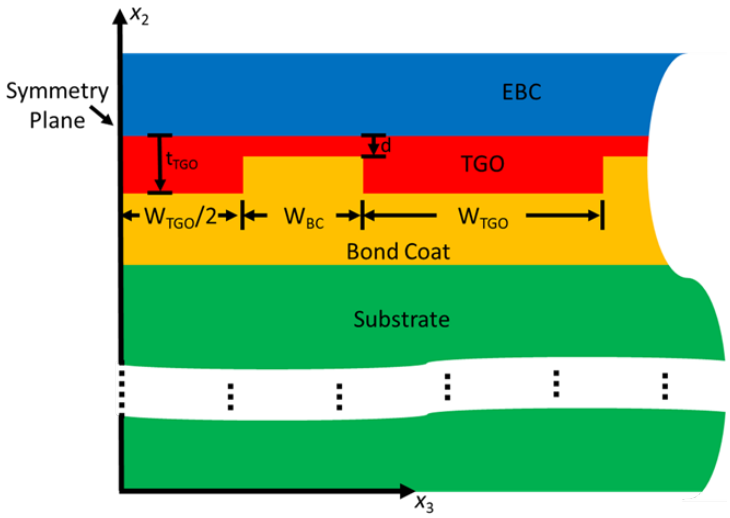

Figure 13.—Schematic showing the geometry of non-uniform TGO layer in a four-layer EBC system.

As was done before with the three-layer system, a non-uniform TGO layer with R = 0.75 was analyzed for two maximum TGO thicknesses: a 4 μm (thin) and a 16 μm (thick) TGO layer. The results for only the thick TGO layer are presented here for the sake of comparison with the results from three-layer systems. The results from thin TGO layer showed very similar trends. Figure 14(a) shows the maximum in-plane tensile stress vs. the crack spacing in the TGO layer. Figure 14(b) to (e) show the TGO layer mesh discretization along with the corresponding in-plane stress state for the undamaged and damaged TGO with 40, 20, and 10 μm crack spacing, respectively. As observed before, when the crack spacing is around 20 μm, cracks start influencing or interacting with each other. At crack spacing of 10 μm maximum tensile stresses near the edges are around 200 MPa. As before, some critical distance is needed (akin to shear-lag theory) for enough in-plane stresses to develop to cause continued cracking.

In this case also, with non-uniform TGO layers, both peel and shear stresses increase significantly with non-uniformity, whether the TGO is undamaged (see Figure 15) or damaged (see Figure 16). Note, in both figures the dashed lines are associated with the thin (4 μm) TGO layer while the solid is associated with the thick (16 μm) TGO layer. Figure 15 shows similar trends that were observed in three-layer system, i.e., non-uniformity causes significant peel and shear stresses even in the absence of any damage. Peel and shear stresses also increase as the TGO thickness grows with time. Figure 16 shows as the damage in introduced in the TGO layer in the form of vertical cracks, peel and shear stresses increase further. Even in the case of uniform TGO layer (R = 1) but with damage, there are peel and shear stresses but as the non-uniformity increases, these stresses can become 4 to 6 times the values when R = 1. It is likely that as the TGO thickness reaches some critical value, the peel stress is high enough to initiate delamination type (horizontal) crack and there are enough shear stresses to drive that crack to cause spallation. It is also observed, as before in the low temperature system, that even though the presence of vertical cracks in TGO layer enhances the peel and shear stresses, the presence of non-uniformity itself is still the primary reason for high peel and shear stresses.

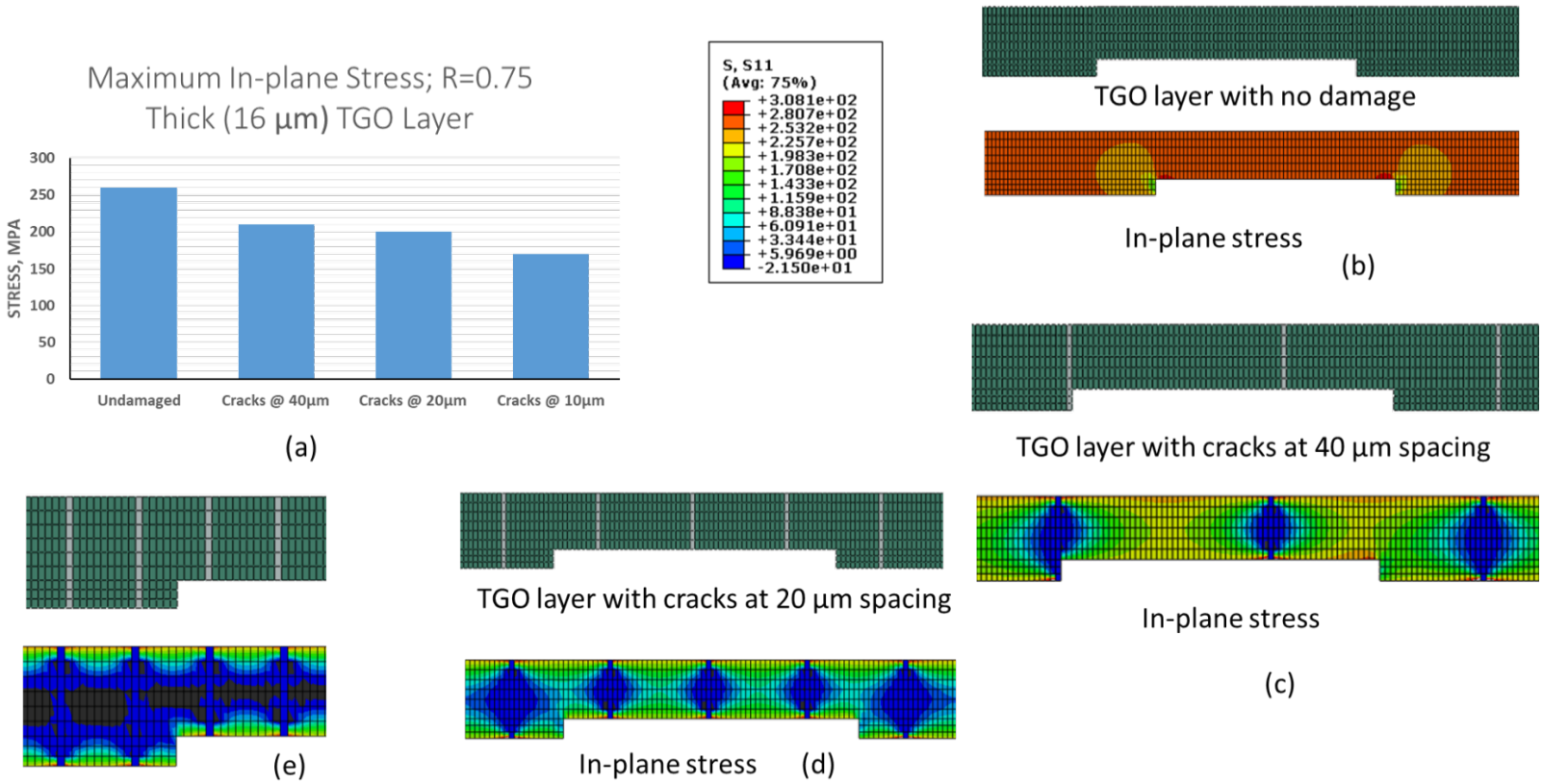

Figure 14.—Maximum in-plane stress in the uniform thick TGO four-layer system (elements representing cracks are shown in gray). (a) Maximum in-plane stress vs. crack spacing. (b) TGO layer discretization with no damage and the resulting in-plane stress state. TGO layer with a crack spacing of (c) 40 μm, (d) 20 μm, and (e) 10 μm and the corresponding resulting in-plane stress contours.

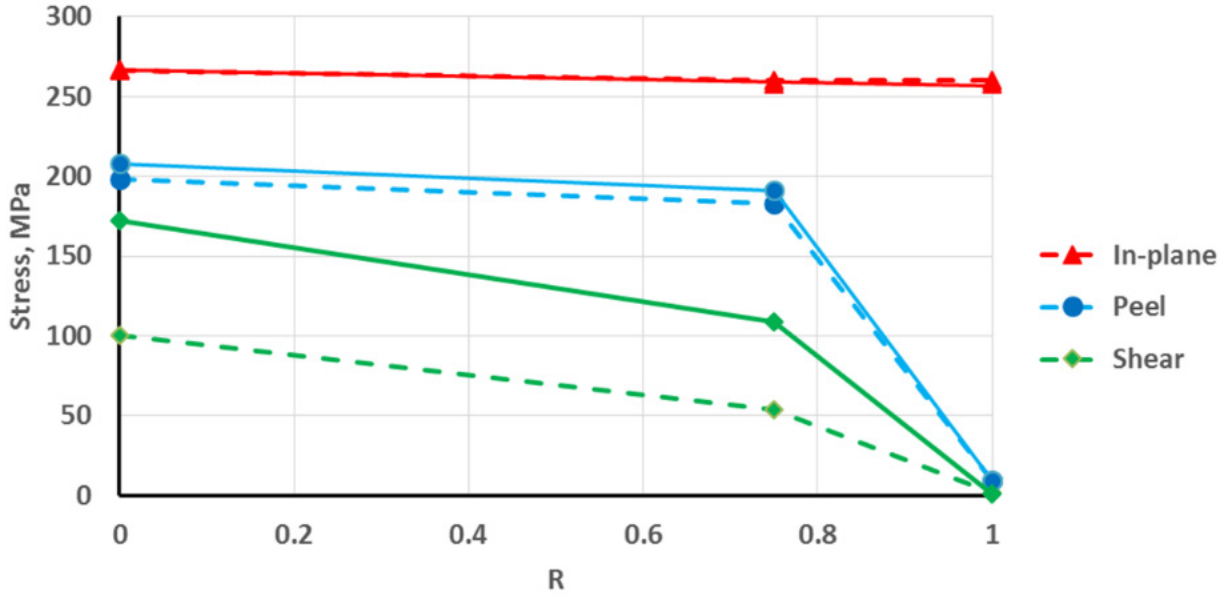

Figure 15.—Maximum stresses in the TGO layer. No damage assumed in TGO layer. Solid lines represent thick (16 μm) TGO and dash line represent thin (4 μm) TGO.

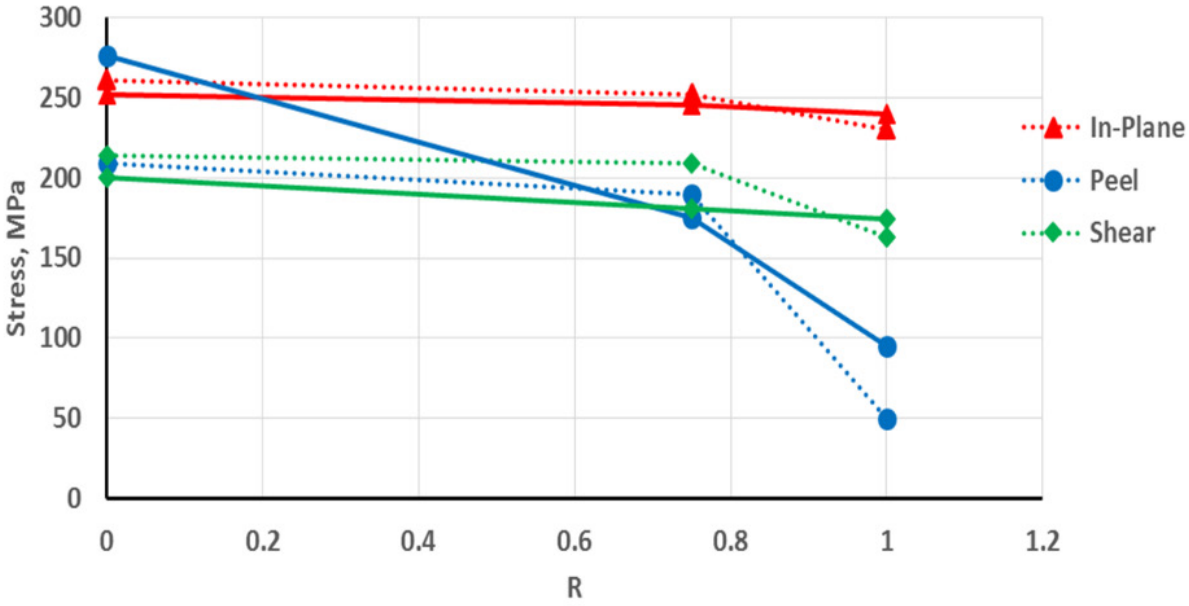

Figure 16.—Maximum stresses in TGO layer. Vertical cracks in TGO layer at a 10 μm spacing. Solid lines represent thick (16 μm) TGO and dash lines represent thin (4 μm) TGO.

General Comments

Figure 17 shows comparison of maximum stresses in the three- and four-layer systems as a function of non-uniformity represented by the parameter, R. No damage in the form of vertical cracks was assumed in these simulations. Solid lines represent four layer and dash lines represent the three-layer system in this figure. Results indicate that the in-plane tensile stress and shear stress are almost identical

in both systems. However, peel stress is approximately 10 percent lower in the three-layer system as compared to that in the four-layer system. Presence of the bond coat seems to help lower peel stress. Since the time effects have not been considered in the present study and the silicon bond coat being perhaps the most creep prone material in the system, the presence of a bond coat should help further reduce the stresses in the EBC system.

Figure 18 shows another perspective to look at the differences between three and four-layer EBC systems. This figure shows the maximum peel stress in the two systems. Both systems have been modeled with 10 μm spaced vertical cracks in the TGO layer. It is also assumed that the TGO layer has a severe non-uniformity (R = 0). Results indicate that when a bond coat layer is added (four-layer system), there is a decrease in peel stress as compared to the stress state with no bond coat layer (three-layer system). This suggests that for a critical failure stress (or equivalently a critical TGO thickness), the silicon bond coat enables thicker TGO layer to be obtained prior to failure. Consequently, coatings with a silicon bond coat layer should have longer life. Obviously, this assumes that the TGO that grows out of a silicon bond coat has the same properties as a TGO that grows out from a SiC substrate.

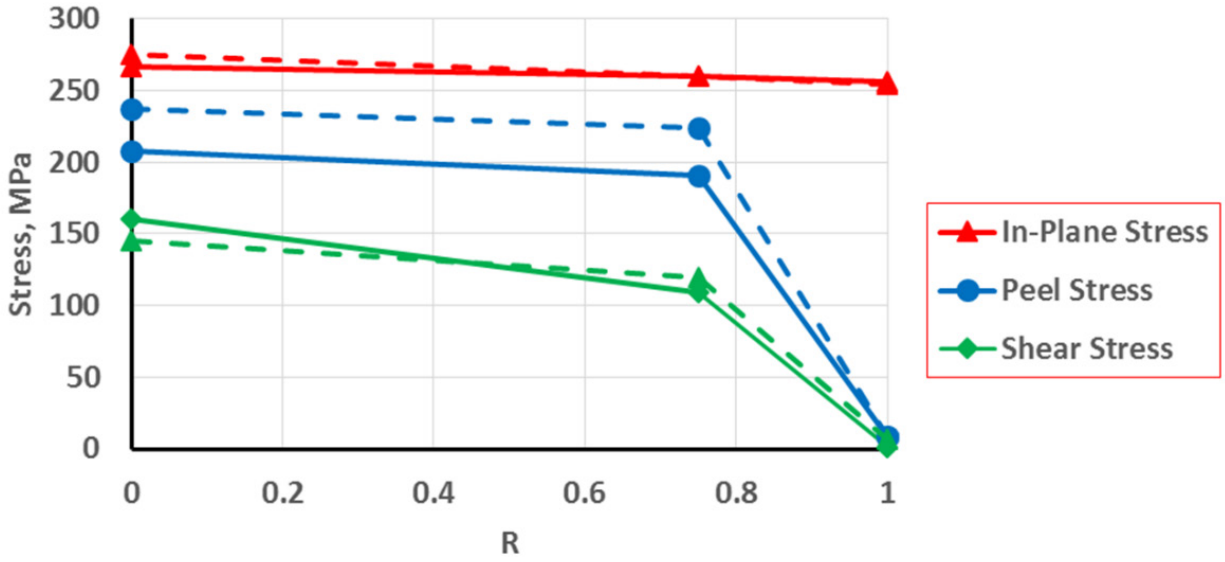

Figure 17.—Comparison of maximum stresses in three- and four-layer systems with undamaged TGO layer. Nominal thickness of TGO layer is 16 μm. Solid lines represent four-layer and dash lines represent three-layer system.

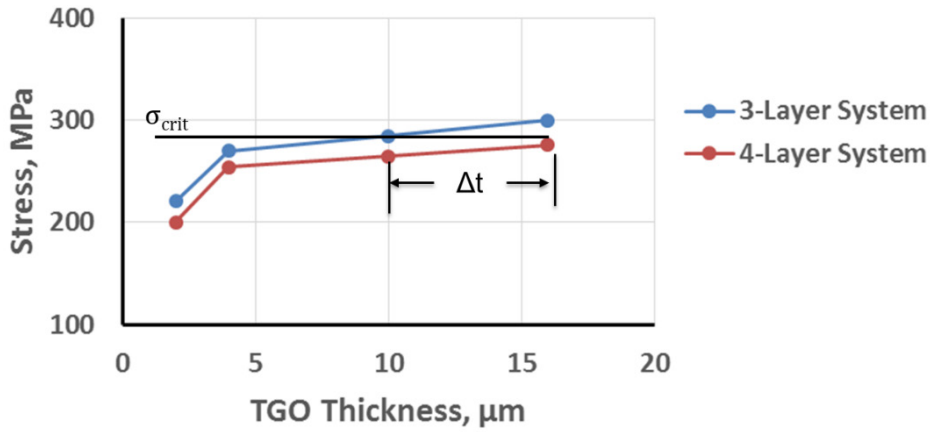

Figure 18.—Peel (2-2) stresses in discontinuous TGO layer with R = 0 and 10 μm spaced cracks.

Conclusions

In this study, a three-layer (EBC/TGO/Substrate) and a four-layer (EBC/TGO/Bond Coat/Substrate) system were analyzed subject to an isothermal cooldown. The influence of two TGO thicknesses for both uniform and non-uniform TGO layers was considered. The analyses attempted to identify and assess how the resulting driving forces (stresses) develop and evolve with respect to damage, thickness and uniformity of the TGO layer. In general, the results for both three- and four-layer systems were very similar.

Results indicate that for uniform thickness TGO layers with no damage, the stress state was independent of the thickness of the TGO layer. There were significant in-plane stresses, but peel and shear stresses are negligible. When damage was introduced in the form of vertical cracks as present in real systems, significant peel and shear stresses developed. Results also indicate that if the average experimentally observed crack spacing in the TGO layer is 10 μm, then the tensile strength of the TGO material (given the current idealization) should be around 200 MPa. In the case of non-uniform TGO layer thicknesses, even a slight non-uniformity in the thickness resulted in significant peel and shear stresses increasing the possibility of delamination and spallation of the EBC when a critical thickness is reached. In addition, when damage was introduced in the form of vertical cracks and when the cracks aligned with the edge of the non-uniformity, there was an increase in peel and shear stresses above and beyond that due to non-uniformity alone, further increasing the possibility of delamination and spallation. The actual cracks, the associated singularity and stress intensity etc. are not explicitly modeled here. In real systems, crack growth and material resistance interact to either cause ultimate failure due to uncontrollable growth or they get arrested and damage saturates. However, simulations shown above indicate that once a vertical crack develops in the TGO layer, it is likely to grow instantaneously due to the presence of high stresses at crack tip. In most situations, the highest TGO stresses occurred at the TGO/EBC interface except for the case when the non-uniformity in the TGO thickness was introduced, at which point the highest stresses occurred at the TGO/substrate interface at the middle of the undulation. In real systems, non-uniformity of the layers and most likely damage will always be present, both of which cause significant peel and shear stresses which in turn will cause delamination initiation and propagation at highest stress locations. The presence of damage (vertical cracks caused by in-plane stresses) increases the peel and shear stresses that are present due to non-uniformity. However, the presence of non-uniformity itself is still the main factor influencing the magnitude of peel and shear stresses. As TGO thickness increases with exposure time, a critical value will be reached whereupon peel and/or shear stresses will exceed the material resistance (strength) and lead to EBC failure. Results also indicate that the presence of a silicon bond coat layer reduces the driving forces. For a given critical failure stress, a silicon bond coat in a four-layer system enables a thicker TGO and thus increased life prior to spallation. It is also very important to note that when characterizing constituents or interfacial strengths, one should account for localization features such as damage, microstructures, residual stress effects, etc. Future work will address the growth rate of the TGO, the anisotropic material properties of the coating, creep/relaxation of various constituents at high temperature, any volumetric and phase changes as well as the constituent material and interfacial bond strength.

References

1. Zok, F.W. 2016. “Ceramic-matrix Composites Enable Revolutionary Gains in Turbine Engine Efficiency”. American Ceramic Society Bulletin, 95(5).
2. Lee, K.N. 2015. “Environmental Barrier Coatings for SiC_F/SiC”. Ceramics Matrix Composites: Materials, Modeling and Technology. First Edition. Edited by Narottam P. Bansal and Jacques Lamon, John Wiley & Sons, Inc.
3. Lee, K.N. 2018. “$Yb_2Si_2O_7$ Environmental Barrier Coatings with Reduced Bond Coat Oxidation Rates via Chemical Modifications for Long Time”. *J. Am. Ceram. Soc.*, 2018;00:1-15, https://doi.org/10.1111/jace.15978.
4. Lee, K.N. 2000. “Current Status of Environmental Barrier Coatings for Si-Based Ceramics.” Surface and Coatings Technology, 133-134:1-7.
5. Ricks, T.M., Arnold, S.M., and Harder, B.J. 2018. “Coupled Thermo-mechanical Modeling of the Influence of Thermally Grown Oxide Layer in an Environemental Barrier Coating System”. Proc. 33rd American Society of Composites Annual Technical Conference, September 24-26, 2018, Seattle, WA.
6. Aboudi, J., Pindera, M-J, and Arnold, S.M. 1999. “Higher-Order Theory For Functionally Graded Materials”. Compos. B, 30:777-832.
7. Dassault Systems Simulia Corp. 2014: ABAQUS Analysis User’s Manual, Version 6.14-1.